Integrated crustal–geological cross-section of Ellesmere Island

R. STEPHENSON[1]*, K. PIEPJOHN[2], C. SCHIFFER[3], W. VON GOSEN[4], G. N. OAKEY[5] & G. ANUDU[1]

[1]*School of Geosciences, Geology and Petroleum Geology, Meston Building, King's College, University of Aberdeen, Aberdeen AB24 3UE, UK*

[2]*Bundesanstalt für Geowissenschaften und Rohstoffe (BGR), 30655 Hanover, Germany*

[3]*Department of Earth Sciences, Durham University, Durham DH1 3LE, UK*

[4]*Geozentrum Nordbayern, Friedrich-Alexander-Universität Erlangen-Nürnberg, 91054 Erlangen, Germany*

[5]*Geological Survey of Canada Atlantic, Halifax, Nova Scotia, Canada*

**Correspondence: r.stephenson@abdn.ac.uk*

Abstract: The crustal seismic velocity model (based on receiver functions) of Ellesmere Island and the structural geological cross-section of Ellesmere Island, both documented and discussed elsewhere in this volume, are here integrated into a crustal-scale transect crossing all the main tectonic domains. The velocity model satisfies much of the observed gravity field, but implies minor modifications with potentially important implications for characterizing the lower crust over the transect. The crust of the Pearya Terrane includes a high-velocity and high-density lower crustal body, suggested to represent a mafic underplate linked to the emplacement of the High Arctic Large Igneous Province. A similar body also lies directly beneath the Hazen Plateau, but this is more likely to be inherited from earlier tectonic stages than to be linked to the High Arctic Large Igneous Province. A large-scale basement-involving thrust, possibly linked to a deep detachment of Ellesmerian age, lies immediately south of the Pearya Terrane and forms the northern backdrop to a crustal-scale pop-up structure that accommodates Eurekan-aged shortening in northern Ellesmere Island. The thickest crust and deepest Moho along the transect are below the Central Ellesmerian fold belt, where the Moho is flexured downwards to the north to a depth of about 48 km beneath the load of the structurally thickened supracrustal strata of the fold belt.

Piepjohn & von Gosen (this volume, in press and references cited therein) have summarized the results of their field seasons of mapping in this volume and elsewhere. Concurrently, the Ellesmere Island Lithosphere Experiment (ELLITE) broadband passive seismological array has been deployed on Ellesmere Island (Stephenson *et al.* 2013) and the receiver functions computed from the recorded teleseismic data have been used by Schiffer *et al.* (2016) to produce, for the first time, a two-dimensional velocity model of the crust of Ellesmere Island, crossing the strike of the Palaeozoic Ellesmerian Orogen with its overprinted Eurekan (Cenozoic) structural elements. The latter has been expanded in this volume and linked with other geophysical data on and around Ellesmere Island to infer maps of the Moho depth, the thickness of the supracrustal (meta) sedimentary layer and, from these, the thickness of the crystalline crust for Ellesmere and Axel Heiberg islands (Schiffer *et al.* 2017). The locations of the structural cross-section segments and the crustal velocity structure profile are shown on Figure 1, which also provides a regional geological map of the study area.

In this paper, the velocity model of Schiffer *et al.* (2016) is used as a base for a density model of the gravity field of Ellesmere Island. The resulting model is then integrated with the geological cross-section of Piepjohn & von Gosen (this volume, in press) to provide a crustal-scale integrated geological–geophysical two-dimensional model of the crust of Ellesmere Island. The geometries of the geophysical models are compared with the mapped kinematics of upper crustal deformation to make inferences about how the crustal structure of Ellesmere Island has been formed by the tectonic events recorded in the geology. In turn, the integrated crustal and shallow depth information may indicate if and how the crustal structure – of which at least some is older than the Cenozoic – has controlled or defined the peculiarities of Eurekan deformation and its relationship with Ellesmerian and older tectonics (e.g. Heron *et al.* 2015).

From: Pease, V. & Coakley, B. (eds) *Circum-Arctic Lithosphere Evolution*. Geological Society, London, Special Publications, **460**, https://doi.org/10.1144/SP460.12

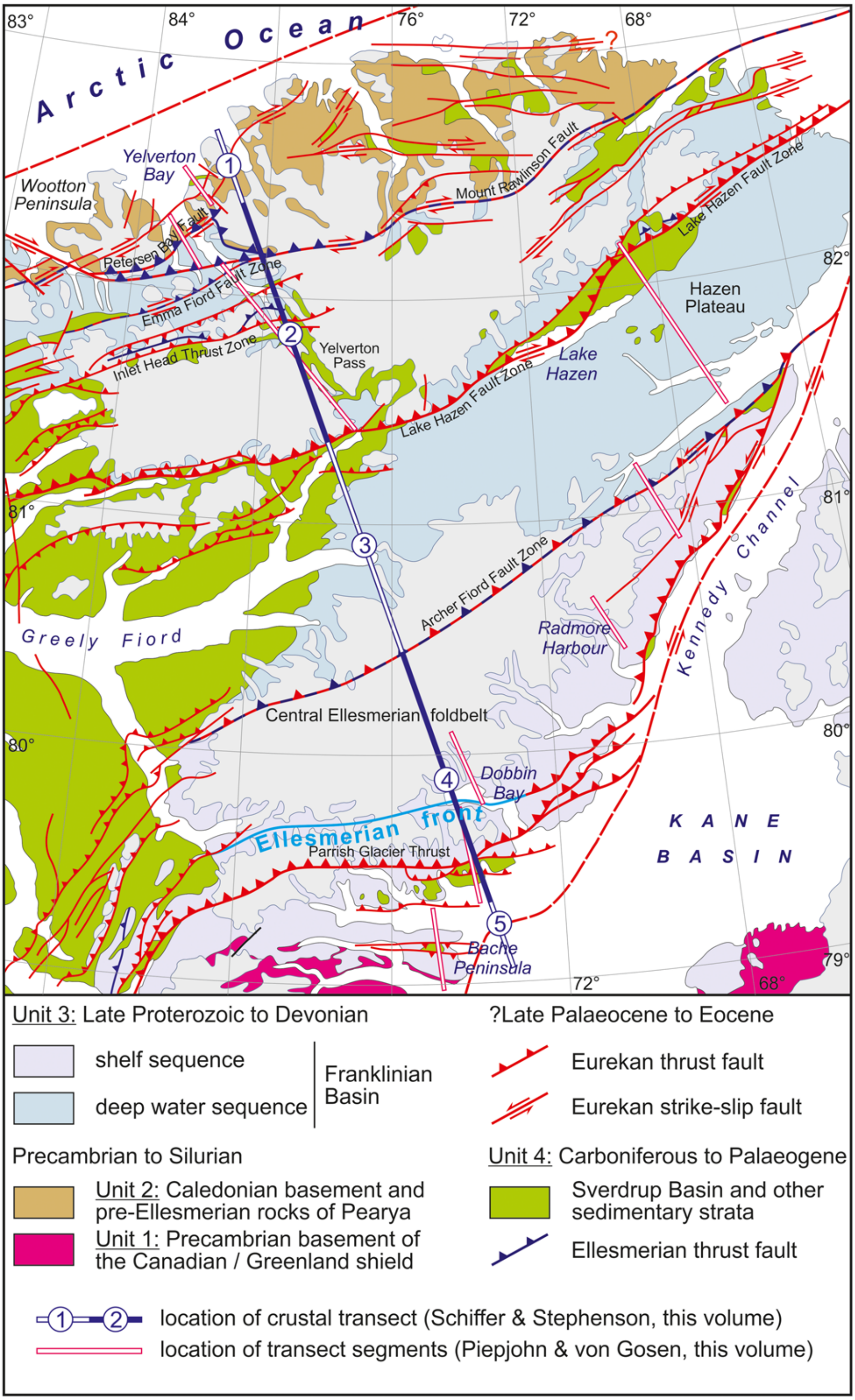
Arctic Ocean
Yelverton Bay
Wootton Peninsula
Petersen Bay Fault
Emma Fiord Fault Zone
Inlet Head Thrust Zone
Mount Rawlinson Fault
Lake Hazen Fault Zone
Yelverton Pass
Hazen Plateau
Lake Hazen
Archer Fiord Fault Zone
Greely Fiord
Radmore Harbour
Kennedy Channel
Central Ellesmerian foldbelt
Dobbin Bay
Ellesmerian front
Parrish Glacier Thrust
KANE BASIN
Bache Peninsula
Unit 3: Late Proterozoic to Devonian
shelf sequence
deep water sequence
Franklinian Basin
Precambrian to Silurian
Unit 2: Caledonian basement and pre-Ellesmerian rocks of Pearya
Unit 1: Precambrian basement of the Canadian / Greenland shield
?Late Palaeocene to Eocene
Eurekan thrust fault
Eurekan strike-slip fault
Unit 4: Carboniferous to Palaeogene
Sverdrup Basin and other sedimentary strata
Ellesmerian thrust fault
location of crustal transect (Schiffer & Stephenson, this volume)
location of transect segments (Piepjohn & von Gosen, this volume)

Geological setting

The northern continental margin of the North American plate on Ellesmere Island consists of four major structural or sedimentary units (Fig. 1). Subsequent to intense deformation and metamorphism in the Precambrian, northern Ellesmere Island and north Greenland were affected by the Palaeozoic Ellesmerian Orogeny and Cenozoic Eurekan deformation (e.g. Thorsteinsson & Tozer 1957, 1960, 1970; Stuart Smith & Wennekers 1979; Trettin 1991*a*).

The first and oldest unit (Unit 1; Fig. 1) is formed by Precambrian crystalline crust of the ancient Laurentian proto-continent, now exposed in the Greenland–Canadian Shield (e.g. Frisch 1983). In the southern part of the area covered by the crustal transect, the crystalline basement is in places overlain by clastic sedimentary rocks of the Mesoproterozoic Thule Basin (e.g. Dawes 1976; Frisch 1983).

Unit 2 (Fig. 1) comprises what is thought to be an exotic crustal fragment, the Pearya Terrane, in the northern part of Ellesmere Island (Schuchert 1923). This terrane is characterized by a different pre-Early Carboniferous evolution from the northern margin of Laurentia and consists of Precambrian basement rocks, metamorphosed Neoproterozoic to Palaeozoic sedimentary rocks and Palaeozoic volcaniclastic rock units (e.g. Trettin 1991*b*; von Gosen *et al.* 2012). The Pearya Terrane was affected by the mid-Ordovician M'Clintock Orogeny, evidence of which is absent elsewhere along the transect. It is thought to have docked to the northern Laurentian margin during the Ellesmerian Orogeny (e.g. Klaper 1992; Mayr *et al.* 1994; Piepjohn *et al.* 2000, 2013), although Hadlari *et al.* (2014) suggested that it may have originated as a fragment of Laurentia that had earlier been rifted away and was only ever separated from Laurentia by a deep marine basin rather than an oceanic domain.

The crystalline and sedimentary rocks of Unit 1 are overlain by the >8 km thick Neoproterozoic to Devonian succession of the Franklinian Basin (Stuart Smith & Wennekers 1979; Dewing *et al.* 2004), which formed the northern passive continental margin of Laurentia during that time. The Franklinian Basin (Unit 3; Fig. 1) can be divided into a southern shelf sequence and a northern deep water sequence (Stuart Smith & Wennekers 1979). The shelf sequence is characterized by a heterogeneous succession of fine- and coarse-grained clastic sediments, evaporites and limestones, whereas the deep water sequence is dominated by fine-grained sediments and monotonous turbidites (e.g. Trettin *et al.* 1991). These deep water sediments of Unit 3 south of the Lake Hazen Fault Zone and north of the Archer Fiord Thrust Zone (Fig. 1), forming the Hazen Plateau, are deformed by NE–SW-trending, tight folds with subvertical axial planes. This belt was called the Hazen Fold Belt by Trettin (1991*a*, *b*) or the Hazen Stable Block by Okulitch & Trettin (1991), a term that was later adopted by Oakey & Stephenson (2008) in discussing the gravity field of the area.

The evolution of the Franklinian Basin was terminated by the earliest Carboniferous with the formation of the Ellesmerian Orogeny (Thorsteinsson & Tozer 1970); it consists of a >350 km wide fold–thrust belt with kilometre-scale anticlines and synclines and subordinate thrust zones (Piepjohn & von Gosen, this volume, in press). The Ellesmerian fold–thrust belt on Ellesmere Island is most probably underlain by a deep-seated detachment (Harrison 2008; Piepjohn *et al.* 2008).

The Sverdrup Basin (Unit 4; Fig. 1) formed after the end of the Ellesmerian Orogeny, starting in the Carboniferous with the deposition of clastic sediments on top of the eroded, deformed and folded Franklinian Basin deposits (Thorsteinsson & Tozer 1970). Carboniferous to Lower Triassic sediments of the Sverdrup Basin overlie the different rock units of the Pearya Terrane, strongly supporting the docking of Pearya against the Franklinian Basin prior to this time. The Sverdup Basin contains up to 16 km of Carboniferous–Upper Cretaceous and Palaeogene rocks (e.g. Balkwill 1978; Embry & Beauchamp 2008).

The development of the Sverdrup Basin terminated in the Eocene (Ricketts & Stephenson 1994). The northern margins of Ellesmere Island and Greenland, the western margin of Spitsbergen and the region along Nares Strait (comprising the Kane Basin and Kennedy Channel within the area seen on Fig. 1) were affected by a complex system of compressional and strike-slip tectonics related to the opening of the Labrador Sea and Baffin Bay, the north Atlantic Ocean and, eventually, the Eurasian Basin (e.g. Tessensohn & Piepjohn 2000; Nielsen *et al.* 2007; Oakey & Chalmers 2012; Piepjohn *et al.* 2013). Eurekan deformation probably took place for the most part in Eocene times, when

Fig. 1. Geological map of north-central Ellesmere Island subdivided into Units 1–4 (Precambrian to Palaeogene; crystalline basement through uppermost sedimentary strata of the Sverdrup Basin). The map shows the main structures of the Palaeozoic Ellesmerian Orogeny (blue) and Cenozoic Eurekan shortening (red) and locations of the geological transect segments (red double lines; cf. Piepjohn & von Gosen this volume, in press) and projected crustal velocity transect (blue double line; cf. Schiffer & Stephenson this volume, in press), the former projected onto the latter in this paper. Numbers on the latter refer to the geological transect segments discussed in the text and seen on Figure 2b. Ice-covered regions onshore have a light grey fill.

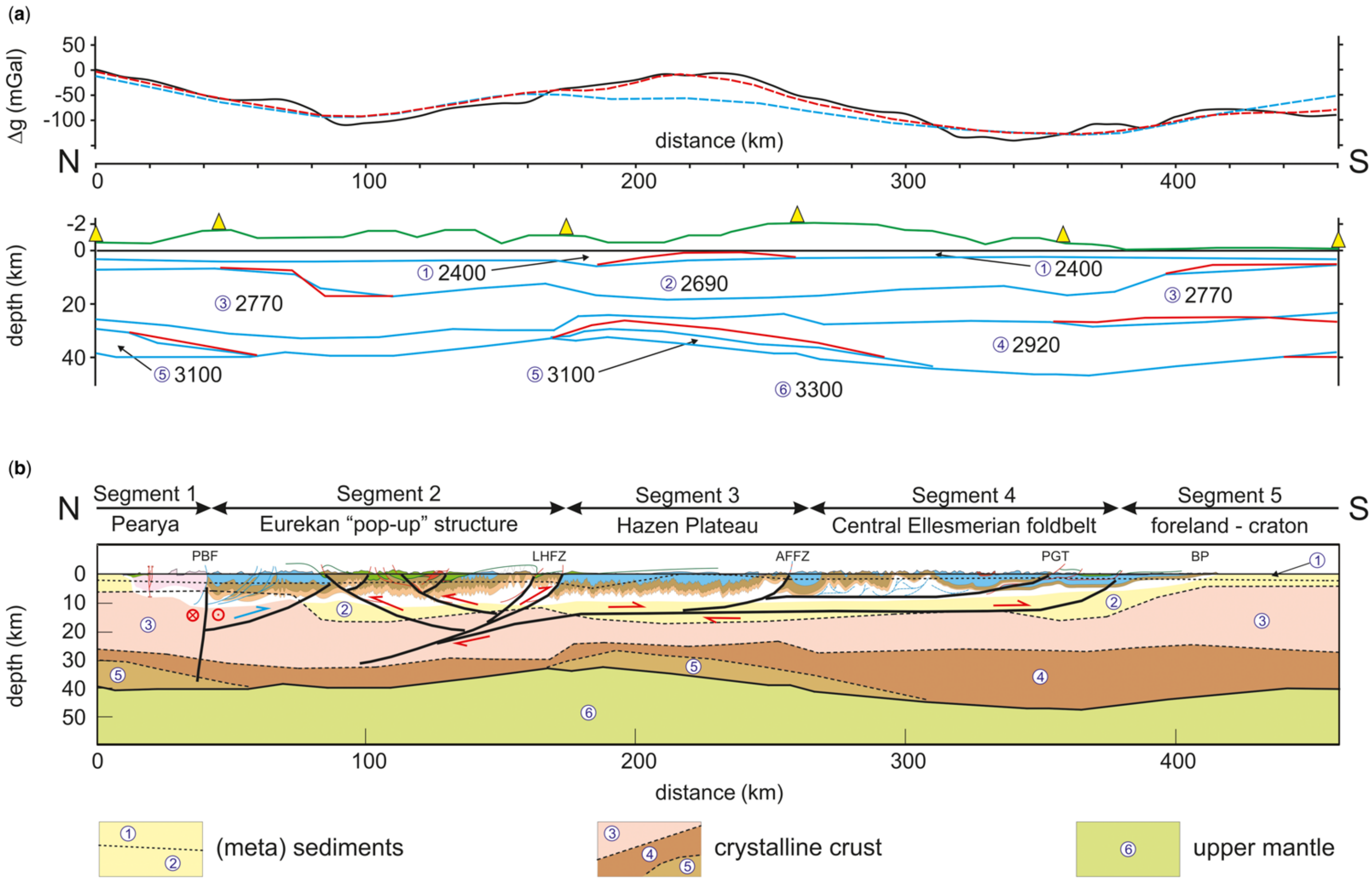
(a)
Δg (mGal)
50
0
-50
-100
distance (km)
N
S
0
100
200
300
400
depth (km)
-2
0
20
40
① 2400
② 2690
① 2400
③ 2770
③ 2770
④ 2920
⑤ 3100
⑤ 3100
⑥ 3300
(b)
Segment 1
Pearya
Segment 2
Eurekan "pop-up" structure
Segment 3
Hazen Plateau
Segment 4
Central Ellesmerian foldbelt
Segment 5
foreland - craton
PBF
LHFZ
AFFZ
PGT
BP
depth (km)
0
10
20
30
40
50
distance (km)
(meta) sediments
crystalline crust
upper mantle

Greenland was a separate plate surrounded by active spreading ridges in the Labrador Sea–Baffin Bay and the north Atlantic Ocean. Eurekan deformation likely took place for the most part in Eocene times, when Greenland was a separate plate surrounded by active spreading ridges in Labrador Sea/Baffin Bay and the north Atlantic Ocean with transform fault systems connecting them west and east of Greenland with the Eurasian Basin (Lepvrier 2000; Tessensohn & Piepjohn 2000; Piepjohn *et al.* 2016). Shortening took place across Ellesmere Island, in particular NW of the Lake Hazen Fault Zone (Fig. 1), which is a zone of SE-directed regional thrusting of Eurekan age (Higgins & Soper 1983; Klaper 1990; Piepjohn *et al.* 2007), and in the Central Ellesmerian fold belt, SE of the Archer Fiord Fault Zone (Fig. 1), which is a zone of SE-vergent regional thrusting of Ellesmerian age reactivated during the Eurekan (Piepjohn *et al.* 2008; Piepjohn & von Gosen this volume, in press). After Eurekan deformation, the common tectonic development of North America and Europe terminated and Europe and North America drifted into their present positions.

Crustal velocity and density model

The two-dimensional velocity model of Schiffer *et al.* (2016) was used as a starting point for a density model of the crust of Ellesmere Island in which different principal crustal features along this two-dimensional profile were tested against observed gravity anomalies. Figure 2a shows the initial model (blue, lower panel) and the observed gravity (black, upper panel) and topography (green, lower panel) along the profile. The gravity and topography profiles were averaged within 40 km wide swathes and five parallel profiles, 10 km apart and centred on the profile location shown on Figure 1, were sampled from the NRCAN gravity database. More details about the distribution of gravity data and other particulars, as well as maps of the gravity and topography, can be found in Oakey & Stephenson (2008).

Schiffer *et al.* (2016) described a classification of S-wave and P-wave velocities to link seismic velocities with lithologies. The velocities were subdivided into layers representative of sediments, metasediments, upper crust, lower crust, high-velocity lower crust and mantle lithosphere (cf. Table 1). The transitions between different layers are diffuse and flexible rather than rigid boundaries as a result of model uncertainty and the natural overlap of velocities of different lithologies.

Table 1. *Velocity ranges inferred from receiver functions by Schiffer et al. (2016) and respective densities based on these for the layers used in the gravity modelling (Fig. 2)*

Layer	Lithology	Velocity ranges (km s^{-1})	Density (kg m^{-3})
1	Sediments	$V_s < 2.6$ $V_p < 4.5$	2400
2	Metasediments	V_s *c.* 2.6–3.1 V_p *c.* 4.5–5.5	2690
3	Upper crust	V_s *c.* 3.1–3.6 V_p *c.* 5.5–6.2	2770
4	Lower crust	V_s *c.* 3.6–3.9 V_p *c.* 6.2–7.2	2920
5	High-velocity lower crust	V_s *c.* 3.9–4.2 V_p *c.* 7.2–7.7	3100
6	Upper mantle lithosphere	$V_s > 4.2$ $V_p > 7.7$	3300

Fig. 2. (**a**) Lower panel: the initial (blue) and final (red modifications) crustal density models, based on the crustal velocity model of Schiffer & Stephenson (this volume, in press) and averaged topography in a 40 km wide corridor centred on the projected location of the crustal velocity model (green line; scale 500% of depth scale). Yellow triangles show the projected locations of ELLITE seismic stations along the profile. Circled numbers refer to model layers as listed in Table 1 and numbers adjacent to these are model layer densities in units of kg m^{-3}; respective seismic velocity ranges determined from receiver functions (e.g. Schiffer *et al.* 2016) for each layer are in Table 1. Upper panel: gravity signatures of the initial and final crustal density models (blue and red dashed lines, respectively) compared with the averaged observed gravity in the 40 km wide corridor along the profile (solid black line). (**b**) The geological transect segments (Piepjohn & von Gosen this volume, in press) projected onto the crustal velocity model (cf. Schiffer & Stephenson (this volume, in press)), here modified according to the final density model shown in part (a). In the geological transect, browns represent Neoproterozoic–Cambrian strata, blue and (minor) reds Ordovician–Silurian and Devonian strata of the Franklinian Basin and green Carboniferous and younger strata of the Sverdrup Basin. Model layers in the crustal geophysical transect correspond to those in Table 1 as indicated by circled numbers on the legend. The boundary between the 'sedimentary' layer and the immediate underlying 'metasedimentary' layer in the velocity and density models is shown by a dashed line. The lower crystalline crust includes high-velocity and high-density bodies (layer 5) beneath segments 1 and 3 (and partly 4), indicated by the greener brown colour. Labelled segments along the model are discussed in the text. As in Figure 1, blue fault labels indicate Ellesmerian structures and red Eurekan structures. Faults and detachments shown as black lines within the crust and overlying (meta) sedimentary successions are purely interpretive, except where they are mapped at the surface (cf. Piepjohn & von Gosen this volume, in press). *Abbreviations*: AFFZ, Archer Fiord Fault Zone; BP, Bache Peninsula; LHFZ, Lake Hazen Fault Zone; PBF, Petersen Bay Fault; PGT, Parrish Glacier Thrust.

Schiffer & Stephenson (this volume, in press) used this classification to construct a structural–lithological interpretation of the two-dimensional velocity model, the geometry of which is used in this study. Each of the lithologies and corresponding velocity ranges were assigned a constant, representative density value (Table 1), resulting in a two-dimensional crustal density model. Densities were chosen on the basis of standard relationships and to be similar to velocity–density assignments from other published studies nearby, particularly Funck *et al.* (2011) and Oakey & Saltus (2016). The two-dimensional model is extrapolated by 150 km at both ends of the profile seen in Figure 2a and also fills the volume within 400 km in both directions perpendicular to the profile to avoid edge effects and to obtain a 2.5-dimensional gravity response. The topography along the swath profile is shown on Figure 2a (green line, with a 500% exaggerated scale compared with depth). This curve gives some representation of how the topography varies along the profile: high in the Pearya Terrane and northern Franklinian Basin (to km 180) and in the Central Ellesmerian fold belt (km 250–380); subdued between these in the Hazen Plateau (km 180–230) and in the cratonic southern part of the profile (beyond km 380). Averaging over a 40 km wide corridor distorts this picture slightly, given the presence of glacially eroded fiords, which are not always parallel to the regional geological strike (Fig. 1).

The gravity signature of the initial model was computed using IGMAS+ software (Schmidt *et al.* 2010) and is indicated by the blue line in Figure 2a. The model was then adjusted to produce the effect indicated by the red line, which is considered to be an acceptable fit to the observed gravity, given the smoothing of the observed data and the degree of extrapolation and regional nature of the initial velocity model. The modifications made to the initial model to achieve the final fit seen in Figure 2a, and the relevant considerations in imposing them, are described in the following text.

The most significant modification addresses that fact that the initial velocity–density model does not satisfactorily replicate the gravity high that characterizes the Hazen Plateau, both in terms of amplitude and spectral composition. Oakey & Stephenson (2008) modelled this anomaly in greater detail (but still at a regional scale), incorporating the inferred supracrustal sedimentary geology of the adjoining Central Ellesmerian fold–thrust belt proposed by Harrison & de Freitas (2007). They concluded, on the basis of both wavelength and amplitude, that high-density, near-surface sediments as well as a deeper, anomalously dense source were required to explain this anomaly. They suggested a shallow Moho, but could not rule out intruded or underplated (ultra)mafic rocks in the lower or middle crust. In keeping with these inferences, shallow as well as deep modifications to the initial model were required in the present study to obtain a reasonable fit with the observed gravity field. First, the sedimentary layer was thinned, in part to near-zero, in the area where, in the initial model, it was mostly interpolated between ELLITE seismic stations (km 190–260). This is appropriate given the deep water lithofacies and degree of deformation and metamorphism of these rocks (e.g. Piepjohn & von Gosen this volume, in press). Second, the receiver functions in this area clearly indicate the presence of a high-velocity lower crustal layer above the Moho (Schiffer *et al.* 2016); its existence is robust in this context and the resolving capabilities of the receiver function models allow its thickness to be increased by several kilometres to match the observed gravity.

Minor modifications were made to the high-velocity lower crustal layer in the northern part of the model (slightly increasing its thickness, with the same argumentation as outlined for the Hazen Plateau; cf. Schiffer *et al.* 2016) and at the metasedimentary layer–crystalline basement layer boundary (minor change to its geometry from km 60 to about km 110, within the resolving capability of the velocity model on which the initial density was based). The effect of these changes on the computed gravity field was small and may be considered as aesthetic rather than necessary. Supplementary minor changes at the sedimentary layer–metasedimentary layer boundary, outwith the resolving capability of the velocity model or the known surface geology, could easily provide a fit to the distinctive feature in the observed gravity at km 60–90. Minor modifications were also made near the southern end of the profile. These are also mainly aesthetic; the goal was to flatten the positive gradient to the south and to suppress the too-high computed gravity south of km 420.

Integrated geological and crustal velocity model: discussion

Figure 2b shows the combined structural transect of Piepjohn & von Gosen (this volume, in press superimposed on the crustal structure model modified from the seismic velocity model of Schiffer *et al.* (2016) to fit the regional gravity anomalies. This 460 km long NNE–SSW crustal transect through northern and central Ellesmere Island is discussed in terms of five major segments, following the division introduced in Piepjohn & von Gosen (this volume, in press).

The northernmost Segment 1 (Fig. 2b) is represented by the composite Pearya Terrane (Unit 2; Fig. 1), which consists of Mesoproterozoic gneisses and metasediments and Neoproterozoic to Palaeozoic metasediments in the vicinity of the crustal transect (cf. Mayr & Trettin 1996). Its southern boundary, at the Petersen Bay Fault (Fig. 2b), is considered to be the boundary between the (exotic) Pearya Terrane and crust of the autochthonous Laurentian continent (e.g. Trettin & Frisch 1987; Klaper & Ohta 1993; Piepjohn *et al.* 2013; Piepjohn & von Gosen this volume, in press) and is expressed as a SE-vergent thrust fault of Ellesmerian Orogeny age (although it may also have been an older structure reactivated at this time; for greater detail, see Piepjohn & von Gosen this volume, in press), which carried the Pearya basement towards the SSE onto Early Palaeozoic turbidites of the Franklinian Basin. This zone was reactivated as a (mainly, but not exclusively, dextral) strike-slip fault system during the Eurekan in the Palaeogene (as indicated on Figure 2b) and the crustal character as a whole differs across it.

There is strong evidence from the geophysical modelling of a high-velocity, high-density lower crustal body beneath Segment 1 (and possibly the northernmost part of Segment 2) and it is likely that this body represents a crustal underplate linked to High Arctic Large Igneous Province (HALIP) magmatism in the contiguous Arctic Ocean (the Alpha Ridge; cf. Døssing *et al.* 2013). Both Anudu *et al.* (2016) and Estrada *et al.* (2016) have explicitly linked the widespread occurrence of Cretaceous and Palaeogene magmatic bodies exposed in this area (as well as those inferred by both research groups within the upper crust) to HALIP and, indeed, the nearest seismic refraction velocity model in the area also presents a high-velocity lower crust (Funck *et al.* 2011; cf. Schiffer & Stephenson this volume, in press for location) comparable with what was inferred in Segment 1 from the ELLITE receiver functions (Schiffer *et al.* 2016).

Segment 2 on Figure 2b, between the Petersen Bay Fault and the Lake Hazen Fault Zone, is characterized by large Ellesmerian fold structures with subvertical fold-axial planes and by Eurekan thrusting (Piepjohn & von Gosen this volume, in press). There is a fairly abrupt deepening of the top crystalline basement in the northern part of Segment 2 (*c.* km 70–80). Based on this and the general prevalence of SSE-directed structures of Ellesmerian age or older in this area, it is suggested that a basement-involving thrust may exist at upper crustal depths. As shown on Figure 2b, it is truncated in the plane of the model cross-section by the Eurekan-aged strike-slip displacements on the Petersen Bay Fault. Sedimentary strata of the post-Ellesmerian Sverdrup Basin are affected by Eurekan deformation in this segment of the transect. In addition, although most Eurekan shortening on Ellesmere Island is more or less SSE-directed, the transport directions in Segment 3 are generally towards the NNW, suggesting the presence of a large-scale pop-up structure in the hanging wall of the Lake Hazen Fault Zone. This is supported by the independently inferred antiformal shape of the top crystalline basement in this area, which has been used as a guide for placing the thrusts that form the deeper expression of the crustal pop-up structure (km 120–180). The gradual deepening to the north of the Moho in this area (km 100–170) is taken to be related to the main crustal underthrust underlying the pop-up zone.

Segment 3 on Figure 2b, corresponding to the Hazen Plateau between the Lake Hazen Fault Zone and the Archer Fiord Fault Zone, is dominated by tight, Ellesmerian-aged folds within monotonous Cambrian to Silurian turbidites of the Franklinian Basin deep water sequence. This area does not show any internal Eurekan deformation and must therefore have been carried passively towards the SSE on top of an inferred detachment at depth (Klaper 1990; Piepjohn *et al.* 2008; Piepjohn & von Gosen this volume, in press). Neither the velocity model nor inferences from the gravity results provides any constraint on the depth of such a detachment and it has been drawn schematically to be within or near the base of what are interpreted from the geophysical data as metasedimentary strata. The crystalline crust beneath Segment 3 is the thinnest anywhere on the transect. Both the upper and lower crustal layers are markedly thinner than either to the north or to the south and this is reflected in a Moho that is shallower than elsewhere along the transect, to as little as *c.* 32 km depth. However, there is also a high-velocity, high-density layer in the lower crust beneath Segment 3 (and the northernmost part of Segment 4).

The high-velocity, high-density layer underlying Segment 3 is essential for explaining the Hazen Plateau gravity high. Equivalently, a more strikingly shallow Moho can also satisfy the gravity high, as proposed by Oakey & Stephenson (2008), but, given the clear evidence for such a body and the fairly well-constrained Moho depth in the receiver functions (cf. Schiffer *et al.* 2016), the present model as seen in Figure 2b is considered to be more plausible. An interesting historical note is the 'Alert Geomagnetic Anomaly' discovered along the strike of the Hazen Plateau in the very early days of geophysical observations on Ellesmere Island and before any gravity measurements were made. Praus *et al.* (1971) attributed it to an elongated conductive body within the lower crust (or upper mantle), such as the high-velocity, high-density body found in the present study, but presumably at a temperature below its Curie point. Given the subdued topography of the Hazen Plateau within Segment 3, it is suggested that its mafic underplate is older than that found under the Pearya Terrane in Segment 1, which has been linked to the HALIP because of the Cretaceous–Palaeogene magmatic rocks occurring there and because of its proximity to the contiguous Alpha Ridge offshore. Cretaceous magmatic rocks do crop out north of Lake Hazen (cf. Fig. 1), along-strike of the Segment 2–Segment 3 boundary *c.* 200 km NE of the transect ('Hassel basalts'; Estrada *et al.* 2016). Although a HALIP link to the inferred high-velocity, high-density lower crustal body in Segment 3 cannot be ruled out, it seems more likely to be associated with the Precambrian formation of the Franklinian continental margin of Laurentia, or possibly the formation of the Sverdrup Basin in the Late Palaeozoic. The distinctive gravity high that is the signature of the high-velocity, high-density body runs the entire length of the Hazen Plateau on Ellesmere Island, from its northeastern tip to Greely Fiord (cf. Fig. 1), which coincides with both the deeper expression of the Franklinian continental margin and the extrapolated axis of Sverdrup Basin rifting. In regard to the latter, it is noted that there are minor magmatic rocks of Permo-Carboniferous age reported in Sverdrup Basin strata in the vicinity of the transect (e.g. Davies & Nassichuk 1991; Embry & Beauchamp 2008).

Segment 4 on Figure 2b, between the Archer Fiord Fault Zone and the Parrish Glacier Thrust, is characterized by broad, kilometre-scale anticlines and synclines with sub-horizontal fold-axial planes of the Central Ellesmerian fold belt, dominantly of Ellesmerian age (Harrison 2008; Piepjohn *et al.* 2008). The minimum depth of the assumed underlying detachment has been estimated by the known thicknesses of the Cambrian to Silurian rock formations in the core of the syncline seen just south of the Archer Fiord Fault Zone. The southernmost large-scale syncline in the hanging wall of the Parrish Glacier Thrust represents the deformation front of the Ellesmerian Orogen (Piepjohn & von Gosen this volume, in press). Folding and thrusting to the south are Eurekan-aged structures. The Moho underlying Segment 4 is the deepest observed along the transect as a whole, down to about 48 km from 32 km in the Hazen Plateau (Segment 3). The deepest Moho is just south of the Parrish Glacier Thrust at about km 370, near the southern limit of Segment 4, where it corresponds directly to the well-constrained receiver function Moho depth determined by Schiffer *et al*. (2016). The Moho in the two-dimensional model is sub-parallel to the metasedimentary layer–upper crystalline crust boundary, which also dips to the north beneath the Central Ellesmerian fold belt. The relationship between the crustal geometry, the geology and the negative gravity anomaly in this area suggests that the crust has been flexed downwards under the load of the thickened fold–thrust belt, as was modelled by Oakey & Stephenson (2008).

Segment 5 on Figure 2b represents the transition of the Eurekan deformation front towards the Eurekan foreland (Piepjohn & von Gosen this volume, in press) and the exposure of Archaean basement south of the transect. The modelled Moho in Segment 5 south of where the northwards flexure begins at *c*. km 430 is at a depth of *c.* 40 km and most of the overlying crust consists of the crystalline basement layers.

Summary and conclusions

The velocity model of the crust of Ellesmere Island determined from receiver functions of earthquake data acquired during the deployment of ELLITE (Stephenson *et al.* 2013; Schiffer *et al.* 2016) was used as the basis of a crustal gravity model crossing the major tectonic/structural domains of Ellesmere Island, running *c.* 460 km NNW–SSE from the vicinity of Yelverton Bay in the north to the vicinity of Bache Peninsula in the south. This crustal structure model has been interpreted by integration with a structural geological transect along the same projected profile location from a series of cross-sections compiled by Piepjohn & von Gosen (this volume, in press). No attempt has been made to incorporate the geometries of the geological units represented in the structural cross-sections into the gravity model given the averaging inherent to the projected crustal velocity model and gravity data. The integrated geological–geophysical model can be considered to some degree a schematic model of the crustal-scale tectonic geometry of Ellesmere Island.

The following key inferences are drawn from the relationships between the shallower structural/geological and deeper geophysical images from north to south.

(1) The crust of the Pearya Terrane of northern Ellesmere Island includes a high-velocity, high-density lower crustal body interpreted to represent a mafic underplate emplaced by the same processes responsible for the emplacement of the Cretaceous–Palaeogene HALIP, which is expressed as numerous mafic intrusions on Ellesmere Island and as Alpha Ridge in its immediate offshore.

(2) The lower crustal high-velocity, high-density body continues marginally to the south beyond the geologically defined southern boundary of the Pearya Terrane (i.e. Petersen Bay Fault), but there is otherwise no strong evidence of a fundamental change in crustal affinity in the deeper geophysical image across this boundary.

(3) There is a fairly abrupt deepening to the south of what is inferred to be the top of the crystalline basement crust south of Petersen Bay Fault (around km 80). This is an area characterized by SSE-directed thrusts of Ellesmerian (and possibly older) age and a speculative interpretation of the basement structure is that it indicates a large-scale basement-involving thrust, possibly linked to a pre-Eurekan deep detachment.

(4) Eurekan shortening in northern Ellesmere Island is expressed mainly as a crustal-scale pop-up structure underlain by, and centred on, a crystalline basement high (at about km 160). The surface expression of the main thrust of this pop-up structure, which is SE-directed, is the Hazen Lake Fault Zone. This is extrapolated to depth as crustal underthrusting to the NNW, reflected by sub-parallel Moho deepening to the north (at about km 100–160). NNW-directed structures to the north of the Hazen Lake Fault Zone (at about km 80–130) represent back-thrusts associated with the crustal-scale pop-up.

(5) The exposed strata in the Hazen Plateau have not been significantly affected by Eurekan-aged deformation, which argues strongly for a Eurekan-aged structural detachment beneath this area. Although there is no direct evidence in the geophysical image of such a detachment, it seems plausible that it is near or at the base of the supracrustal metasedimentary layer identified by the velocity and density models (depth *c.* 12–17 km).

(6) There is strong evidence for the existence of a high-velocity, high-density body in the lower crust directly beneath the Hazen Plateau. This is considered more likely to be inherited from the Early Palaeozoic Franklinian margin or linked to the Late Palaeozoic Sverdrup Basin formation than to be related to HALIP emplacement in the Cretaceous–Palaeogene.

(7) The thickest crust and deepest Moho along the transect is below the Central Ellesmerian fold belt, where the Moho is as deep as 48 km. The crystalline crust as a whole appears to be flexed downwards to the north beneath the load of the structurally thickened supracrustal strata of the fold belt, typical of a foreland basin tectonic setting.

The work reported in this paper was undertaken under the umbrella of CALE. The work on the geological transect was enabled by several CASE (Circum-Arctic Structural Events) expeditions of the Federal Institute for Geosciences and Natural Resources (BGR, Hanover, Germany). The postdoctoral fellowship at Durham University of CS is funded by the Carlsberg Foundation.

References

Anudu, G.K., Stephenson, R.A., Macdonald, D.I.M. & Oakey, G.N. 2016. Geological features of the northeastern Canadian Arctic margin revealed from analysis of potential field data. *Tectonophysics*, **691**, 48–64, https://doi.org/10.1016/j.tecto.2016.03.025

Balkwill, H.R. 1978. Evolution of Sverdrup Basin, Arctic Canada. *American Association of Petroleum Geologists Bulletin*, **62**, 1004–1028.

Davies, G.R. & Nassichuk, W.W. 1991. Carboniferous and Permian history of the Sverdrup Basin, Arctic Islands. *In*: Trettin, H.P. (ed.) *Geology of the Innuitian Orogen and Arctic Platform of Canada and Greenland*. Geology of Canada, **3**. Geological Survey of Canada, Ottawa, 345–367.

Dawes, P.R. 1976. Precambrian to Tertiary of northern Greenland. *In*: Escher, W. & Watt, W.S. (eds) *Geology of Greenland*. Geological Survey of Greenland, Copenhagen, 248–303.

Dewing, K., Harrison, J.C., Pratt, B.R. & Mayr, U. 2004. A probable late Neoproterozoic age for the Kennedy Channel and Ella Bay formations, northeastern Ellesmere Island and its implications for the passive margin history of the Canadian Arctic. *Canadian Journal of Earth Sciences*, **41**, 1013–1025.

Døssing, A., Jackson, H.R., Matzka, J., Einarsson, I., Rasmussen, T.M., Olesen, A.V. & Brozena, J.M. 2013. On the origin of the Amerasia Basin and the High Arctic Large Igneous Province – results of new aeromagnetic data. *Earth and Planetary Science Letters*, **363**, 219–230, https://doi.org/10.1016/j.epsl.2012.12.013

Embry, A. & Beauchamp, B. 2008. Sverdrup basin. *In*: Miall, A. (ed.) *Sedimentary Basins of the World*. Vol. **5**. Elsevier, Amsterdam, 451–471.

Estrada, S., Damaske, D. *et al.* 2016. Multistage Cretaceous magmatism in the northern coastal region of Ellesmere Island and its relation to the formation of Alpha Ridge – evidence from aeromagnetic, geochemical and geochronological data. *Norwegian Journal of Geology*, **96**, 2, https://doi.org/10.17850/njg96-2-03

Frisch, T. 1983. *Reconnaissance Geology of the Precambrian Shield of Ellesmere, Devon and Coburg Islands, Arctic Archipelago: a Preliminary Report*. Geological Society of Canada, Papers, **82-10**, 1–11.

Funck, T., Jackson, H.R. & Shimeld, J. 2011. The crustal structure of the Alpha Ridge at the transition to the Canadian Polar Margin: results from a seismic refraction experiment. *Journal of Geophysical Research: Solid Earth*, **116**, B12101, https://doi.org/10.1029/2011JB008411

Hadlari, T., Davis, W.J. & Dewing, K. 2014. A pericratonic model for Pearya Terrane as an extension of the Franklinian margin of Laurentia, Canadian Arctic. *Geological Society of America Bulletin*, **126**, 182–200.

Harrison, J.C. 2008. Regional variation in structural style, deformation kinematics, and summary of tectonic history, northeast Ellesmere Island. *In*: Mayr, U. (ed.) *Geology of Northeast Ellesmere Island Adjacent to Kane Basin and Nares Strait, Nunavut*. Geological Survey of Canada, Bulletin, **592**, 245–284.

Harrison, J.C. & de Freitas, T.A. 2007. *Geology, Agassiz Ice Cap, Ellesmere Island, Nunavut. Scale 1:125.000*. Geological Survey of Canada, Maps, **2104A**.

Heron, P.J., Pysklywec, R.N. & Stephenson, R. 2015. Intraplate orogenesis within accreted and scarred lithosphere: example of the Eurekan Orogeny, Ellesmere Island. *Tectonophysics*, **664**, 202–213, https://doi.org/10.1016/j.tecto.2015.09.011

Higgins, A.K. & Soper, N.J. 1983. *The Lake Hazen Fault Zone, Ellesmere Island: a Transpressional Upthrust?* Current Research, Part B, Geological Survey of Canada, Papers, **83-1B**, 215–221.

Klaper, E.M. 1990. The mid-Paleozoic deformation in the Hazen fold belt, Ellesmere Island, Arctic Canada. *Canadian Journal of Earth Sciences*, **27**, 1359–1370.

Klaper, E.M. 1992. The Paleozoic tectonic evolution of the northern edge of North America – a structural study of northern Ellesmere Island, Canadian Arctic Archipelago. *Tectonics*, **11**, 854–870.

Klaper, E.M. & Ohta, Y. 1993. Paleozoic metamorphism across the boundary between the Clements Markham fold belt and the Pearya terrane in northern Ellesmere Island, Canadian Arctic Archipelago. *Canadian Journal of Earth Sciences*, **30**, 867–880.

Lepvrier, C. 2000. Drift of Greenland and correlation of Tertiary tectonic events in the West Spitsbergen and Eurekan fold-and-thrust belts. *In*: Roland, N.W. & Tessensohn, F. (eds) *ICAM III – International Conference on Arctic Margins*. Vol. **I**. *Polarforschung*, **68**, 93–100.

Mayr, U. & Trettin, H.P. 1996. *Geological Map of Tanquary Fiord, District of Franklin, 1:250.000*. Geological Survey of Canada, Maps, **1886A**.

Mayr, U., Packard, J.J., Goodbody, Q.H., Okulitch, A.V., Rice, R.J., Goodarzi, F. & Stewart, K.R. 1994. The Phanerozoic geology of Southern Ellesmere and North Kent Islands. *Geological Survey of Canada Bulletin*, **470**, 1–298.

Nielsen, S.B., Stephenson, R.A. & Thomsen, E. 2007. Dynamics of Mid-Palaeocene North Atlantic rifting linked with European intra-plate deformations. *Nature*, **450**, 1071–1074, https://doi.org/10.1038/nature06379

Oakey, G.N. & Chalmers, J.A. 2012. A new model for the Paleogene motion of Greenland relative to North America: plate reconstructions of the Davis Strait and Nares Strait regions between Canada and Greenland. *Journal of Geophysical Research*, **117**, B10401, https://doi.org/10.1029/2011JB008942

Oakey, G.N. & Saltus, R.W. 2016. Geophysical analysis of the Alpha–Mendeleev Ridge complex: characterization of the High Arctic Large Igneous Province. *Tectonophysics*, **691**, 65–84, https://doi.org/10.1016/j.tecto.2016.08.005

Oakey, G.N. & Stephenson, R.A. 2008. Crustal structure of the Innuitian region of Arctic Canada and Greenland from gravity modelling: implications for the Palaeogene Eurekan Orogen. *Geophysical Journal International*, **173**, 1039–1063, https://doi.org/10.1111/j.1365-246X.2008.03784.x

Okulitch, A.V. & Trettin, H.P. 1991. Late Cretaceous-Early Tertiary deformation, Arctic Islands. *In*: Trettin, H.P. (ed.) *Geology of Canada, 3: Geology of the Innuitian Orogen and Arctic Platform of Canada and Greenland*. Geological Survey of Canada (also Geology of North America, Vol. E, Geological Society of America), 467–485.

Piepjohn, K. & von Gosen, W. In press. A structural transect through Ellesmere Island (Canadian Arctic): superimposed Palaeozoic Ellesmerian and Cenozoic Eurekan deformations. *In*: Pease, V. & Coakley, B. (eds) *Circum-Arctic Lithosphere Evolution*. Geological Society, London, Special Publications, **460**, https://doi.org/10.1144/SP460.5

Piepjohn, K., Brinkmann, L., Grewing, A. & Kerp, H. 2000. New data on the age of the uppermost ORS and the lowermost post-ORS strata in Dickson Land (Spitsbergen) and implications for the age of the Svalbardian deformation. *In*: Friend, P.F. & Williams, B.P.J. (eds) *New Perspectives on the Old Red Sandstone*. Geological Society, London, Special Publications, **180**, 603–609, https://doi.org/10.1144/GSL.SP.2000.180.01.32

Piepjohn, K., von Gosen, W., Estrada, S. & Tessensohn, F. 2007. Deciphering superimposed Ellesmerian and Eurekan deformation, Piper Pass area, northern Ellesmere Island (Nunavut). *Canadian Journal of Earth Sciences*, **44**, 1439–1452.

Piepjohn, K., von Gosen, W., Tessensohn, F. & Saalmann, K. 2008. Ellesmerian fold-and-thrust belt (northeast Ellesmere Island, Nunavut) and its Eurekan overprint. *In*: Mayr, U. (ed.) *Geology of Northeast Ellesmere Island Adjacent to Kane Basin and Nares Strait, Nunavut*. Geological Survey of Canada, Bulletin, **592**, 285–303.

Piepjohn, K., von Gosen, W., Läufer, A., McClelland, W.C. & Estrada, S. 2013. Ellesmerian and Eurekan fault tectonics at the northern margin of Ellesmere Island (Canadian High Arctic). *Zeitschrift der Deutschen Gesellschaft für Geowissenschaften*, **164**, 81–105.

Piepjohn, K., von Gosen, W. & Tessensohn, F. 2016. The Eurekan deformation in the Arctic: an outline. *Journal of the Geological Society*, **173**, 1007–1024, https://doi.org/10.1144/jgs2016-081

Praus, O., DeLaurier, J.M. & Law, L.K. 1971. The extension of the alert geomagnetic anomaly through Northern Ellesmere Island, Canada. *Canadian Journal of Earth Sciences*, **8**, 50–64, https://doi.org/10.1139/e71-003

Ricketts, B.D. & Stephenson, R.A. 1994. The demise of Sverdrup Basin: late Cretaceous–Palaeogene sequence stratigraphy and forward modelling. *Journal of Sedimentary Research*, **64**, 516–530.

Schiffer, C. & Stephenson, R.A. In press. Regional crustal architecture of Ellesmere Island, Arctic Canada. *In*: Pease, V. & Coakley, B. (eds) *Circum-Arctic Lithosphere Evolution*. Geological Society, London, Special Publications, **460**, https://doi.org/10.1144/SP460.8

Schiffer, C., Stephenson, R., Oakey, G.N. & Jacobsen, B.H. 2016. The crustal structure of Ellesmere Island, Arctic Canada – teleseismic mapping across a remote intraplate orogenic belt. *Geophysical Journal International*, **204**, 1579–1600, https://doi.org/10.1093/gji/ggv539

Schiffer, C., Tegner, C., Schaeffer, A.J., Pease, V. & Nielsen, S.B. 2017. The High Arctic geopotential stress field and its implications for the geodynamic Evolution. *In*: Pease, V. & Coakley, B. (eds) *Circum-Arctic Lithosphere Evolution*. Geological Society, London, Special Publications, **460**. First published online April 13, 2017, https://doi.org/10.1144/SP460.6

Schmidt, S., Götze, H.J., Fichler, C. & Alvers, M. 2010. IGMAS+ – a new 3D gravity, FTG and magnetic modeling software. *In*: *Konferenzband GEO-INFORMATIK 2010 Die Welt Im Netz, Herausgeber*. Akademische Verlagsgesellschaft, 57–63.

Schuchert, C. 1923. Sites and nature of the North American geosynclines. *Geological Society of America Bulletin*, **34**, 151–229.

Stephenson, R., Oakey, G.N., Schiffer, C. & Jacobsen, B.H. 2013. *Ellesmere Island Lithosphere Experiment (ELLITE): Eurekan Basin Inversion and Mountain Building, Ellesmere Island, Nunavut*. Geological Survey of Canada, Current Research, **2013-21**.

Stuart Smith, J.H. & Wennekers, J.H.N. 1979. Geology and hydrocarbon discoveries of Canadian Arctic Islands. *American Association of Petroleum Geologists Bulletin*, **61**, 1–27.

Tessensohn, F. & Piepjohn, K. 2000. Eocene compressive deformation in Arctic Canada, North Greenland and Svalbard and its plate tectonic causes. *In*: Roland, N.W. & Tessensohn, F. (eds) *ICAM III – International Conference on Arctic Margins*. Vol. **I**. *Polarforschung*, **68**, 121–124.

Thorsteinsson, R. & Tozer, E.T. 1957. Geological investigation in Ellesmere and Axel Heiberg Islands. *Arctic*, **10**, 2–31.

Thorsteinsson, R. & Tozer, E.T. 1960. *Summary Account of Structural History of the Canadian Arctic Archipelago Since Precambrian Time*. Geological Survey of Canada, Papers, **60-7**, 1–23.

Thorsteinsson, R. & Tozer, E.T. 1970. Geology of the arctic archipelago. *In*: Douglas, R.J.W. (ed.) *Geology and Economic Minerals of Canada*. Geological Survey of Canada, Economic Geology Reports, **1**, 547–590.

Trettin, H.P. 1991*a*. Tectonic framework. *In*: Trettin, H.P. (ed.) *Chapter 4 in Geology of the Innuitian Orogen and Arctic Platform of Canada and Greenland*. Geological Survey of Canada, Geology of Canada, **3**, 59–66.

Trettin, H.P. 1991*b*. Late Silurian–Early Devonian deformation, metamorphism, and granitic plutonism, northern Ellesmere and Axel Heiberg islands. *In*: Trettin, H.P. (ed.) *Geology of the Innuitian Orogen and Arctic Platform of Canada and Greenland*. Geology of Canada, **3**. Geological Survey of Canada, Ottawa, 295–301.

Trettin, H.P. & Frisch, T. 1987. *Bedrock Geology, Yelverton Inlet Map Area, Northern Ellesmere Island. Interim Report and Map (340F, 560D)*. Geological Survey of Canada, Open File Report **1651**.

Trettin, H.P., Mayr, U., Long, G.D.F. & Packard, J.J. 1991. Cambrian to Early Devonian basin development, sedimentation, and volcanism, Arctic Islands. *In*: Trettin, H.P. (ed.) *Geology of the Innuitian Orogen and Arctic Platform of Canada and Greenland*. Geology of Canada, **3**. Geological Survey of Canada, Ottawa, 165–238.

von Gosen, W., Piepjohn, K., McClelland, W.C. & Läufer, A. 2012. The Pearya Shear Zone in the Canadian High Arctic: kinematics and significance. *German Journal of Geosciences*, **163**, 233–249.